Quantifying catchment-scale mixing and its effect on time-varying travel time distributions

Y. van der Velde,[1] P. J. J. F. Torfs,[2] S. E. A. T. M. van der Zee,[3] and R. Uijlenhoet[2]

Received 20 August 2011; revised 7 May 2012; accepted 17 May 2012; published 29 June 2012.

[1] Travel time distributions are often used to characterize catchment discharge behavior, catchment vulnerability to pollution and pollutant loads from catchments to downstream waters. However, these distributions vary with time because they are a function of rainfall and evapotranspiration. It is important to account for these variations when the time scale of interest is smaller than the typical time-scale over which average travel time distributions can be derived. Recent studies have suggested that subsurface mixing controls how rainfall and evapotranspiration affect the variability in travel time distributions of discharge. To quantify this relation between subsurface mixing and dynamics of travel time distributions, we propose a new transformation of travel time that yields transformed travel time distributions, which we call Storage Outflow Probability (STOP) functions. STOP functions quantify the probability for water parcels in storage to leave a catchment via discharge or evapotranspiration. We show that this is equal to quantifying mixing within a catchment. Compared to the similar Age function introduced by Botter et al. (2011), we show that STOP functions are more constant in time, have a clearer physical meaning and are easier to parameterize. Catchment-scale STOP functions can be approximated by a two-parameter beta distribution. One parameter quantifies the catchment preference for discharging young water; the other parameter quantifies the preference for discharging old water from storage. Because of this simple parameterization, the STOP function is an innovative tool to explore the effects of catchment mixing behavior, seasonality and climate change on travel time distributions and the related catchment vulnerability to pollution spreading.

Citation: van der Velde, Y., P. J. J. F. Torfs, S. E. A. T. M. van der Zee, and R. Uijlenhoet (2012), Quantifying catchment-scale mixing and its effect on time-varying travel time distributions, *Water Resour. Res.*, *48*, W06536, doi:10.1029/2011WR011310.

1. Introduction

[2] The probability distribution of the time it takes water from the moment it reaches the surface in the form of rainfall until it reaches the outlet of a catchment is widely used as a fundamental average catchment property [*Kirchner et al.*, 2000; *Lindgren et al.*, 2004; *McGuirre and McDonnell*, 2006; *McDonnell et al.*, 2010]. This travel time distribution characterizes the average discharge behavior of a catchment, provides information about the vulnerability of a catchment to pollution spreading [*Rinaldo and Marani*, 1987; *Destouni and Graham*, 1995; *Persson and Destouni*, 2009; *Visser et al.*, 2009] and is often used to quantify pollutant loads from a catchment to downstream surface and coastal waters [*Destouni et al.*, 2006; *Darracq et al.*, 2010; *Lyon et al.*, 2010]. However, many studies have shown that travel time distributions may vary strongly as function of time due to seasonal and event driven variations in rainfall and evapotranspiration [*Destouni*, 1991; *Van der Velde et al.*, 2010a; *Botter et al.*, 2010, 2011; *McDonnell et al.*, 2010; *Hrachowitz et al.*, 2010; *Rinaldo et al.*, 2011]. This variation compromises the use of a single travel time distribution in studies that use travel time distributions to model stream tracer concentrations at time-scales smaller than the time period for which average travel time distributions can be defined [*Hrachowitz et al.*, 2011]. *Botter et al.* [2011] and *Soulsby et al.* [2009] suggested that subsurface mixing largely controls how weather variability and climate changes are transferred into variability of travel time distributions. However, research aimed at quantifying and parameterizing catchment-scale mixing for real catchments and studies that investigate the relations between subsurface mixing and catchment-scale travel time distributions are still lacking.

[3] Catchment-scale stream water travel time distributions depend on climate, vegetation, topography, and subsurface properties [*Tetzlaff et al.*, 2009, 2011; *Hrachowitz et al.*, 2009a, 2009b; *McGuire et al.*, 2005; *Cardenas*, 2007; *Broxton et al.*, 2009]. *Tetzlaff et al.* [2011] and *Harachowitz et al.* [2009b] concluded based on tracer measurements in Scottish catchments that soil type and flowpath length related

[1]Physical Geography and Quaternary Geology, Stockholm University, Stockholm, Sweden.
[2]Hydrology and Quantitative Water Management Group, Wageningen University, Wageningen, Netherlands.
[3]Soil Physics, Ecohydrology and Groundwater Management Group, Wageningen University, Wageningen, Netherlands.

Corresponding author: Y. van der Velde, Physical Geography and Quaternary Geology, Stockholm University, 106 91 Stockholm, Sweden. (ype.vandervelde@natgeo.su.se)

0043-1397/12/2011WR011310

to drainage intensity are the controlling factors for catchment mean travel times. They found short mean travel times on slopes with shallow soils, while their flattest catchments with relatively deep soils yielded much longer and more constant travel times due to the larger volume of stored groundwater. During large storm events, however, overland flow and other preferential flow routes caused a sharp decline in the mean travel time of these flat catchments. In other parts of the world, with less variation in soil types and steeper topographic gradients, it was found that the effect of gradient on mean travel times is dominant over the effect of soil type [*Tetzlaff et al.*, 2009; *McGuire et al.*, 2005]. Essentially, this was also one of the findings of *Harman and Sivapalan* [2009] based on theoretical considerations. *Hrachowitz et al.* [2009b] showed for Scottish catchments that regional differences in precipitation and evapotransipiration cause differences in mean travel times between catchments as well; in wet catchments with much rainfall, water flows faster through the catchment yielding relatively short mean travel times, while in drier catchments with similar topography and subsurface, water flows slower and travel times are longer. *Rinaldo et al.* [2011] illustrated similar behavior with a conceptual model for travel time dynamics of a single catchment. The impact of weather variability on travel time distributions and its relation to transport of solutes was studied in detail by *Van der Velde et al.* [2010a]. They showed that the dynamics in observed surface water nitrate and chloride concentrations of a small catchment relate strongly to the continuously changing shape of numerically derived travel time distributions. All these studies emphasize the importance of accounting for temporal variability in travel time distributions.

[4] *Niemi* [1977] and *Wierenga* [1977] proposed to transform travel times into cumulative discharge as a function of travel time to relate travel times to the hydrological conditions of a catchment and hence reduce variability of travel time distributions. This transformation yields a smooth travel time distribution, in which variability originating from rainfall is attenuated by the corresponding variability in discharge [see *Fiori and Russo*, 2008]. *Van Ommen et al.* [1989a, 1989b], *Kirchner et al.* [2000] and many others effectively applied this approximation in catchment hydrology when travel times of water are relatively short, fluxes are dominated by a single flow route (discharge) and the catchment storage remains relatively constant. However, in many catchments, evapotranspiration (a second flow route) is a significant flux compared to discharge and both flow routes typically have entirely different travel time distributions as their flow paths are completely different [*Brooks et al.*, 2010]. Hence, *Fiori and Russo* [2008], *Botter et al.* [2011], and *Rinaldo et al.* [2011] emphasized that evapotranspiration may significantly affect stream water travel times and thus should be explicitly accounted for. *Botter et al.* [2011] formulated catchment-scale travel time distribution functions that account for these differences between discharge and evapotranspiration and explicitly address subsurface mixing, but they did not yet apply their equations to real catchments. *Rinaldo et al.* [2011] also avoided the problem of parameterizing incomplete subsurface mixing by assuming perfect mixing of subsurface waters. This assumption, by definition, implies the same travel time distributions for all flow routes leaving a catchment. Since travel time distribution differences between discharge and evapotranspiration have been recognized as a key characteristic of catchments, incorporating incomplete subsurface mixing for real catchments is needed.

[5] The objective of our paper is to introduce a new transformation of travel times that reduces temporal variability in travel time distributions by quantifying mixing of water within a catchment. We test our transformation for the Hupsel Brook agricultural catchment in the Netherlands and evaluate its ability to describe dynamics of travel time distributions and the related dynamics of surface water solute concentrations. Furthermore, we explore effects of different landscapes on subsurface mixing and long term average travel time distributions of stream water.

2. Storage Outflow Probability Function

2.1. Theory of Travel Time Distributions

[6] In solute transport studies it is useful to distinguish between the resident and the flux concentration of solutes [e.g., *Kreft and Zuber*, 1978; *Parker and Van Genuchten*, 1984; *Bloem et al.*, 2008]. The resident concentration quantifies the average solute concentration of water inside a volume of soil, while the flux concentration is the concentration of water that passes a control plane within the soil. For travel time distributions of entire catchments a similar distinction exists: due to incomplete mixing of the water within a catchment, the travel time distribution of water found inside a catchment differs from the travel time distribution of water that exits a catchment by discharge, evapotranspiration, extractions or other flow routes. Hence, we adopt the terms *resident travel time distribution* and *flux travel time distribution* to distinguish between both distributions [*McDonnell et al.*, 2010; *Kreft and Zuber*, 1978]. Complete analytical solutions for the resident travel time and the flux travel time distributions are given by the Master Equations of *Botter et al.* [2011]. In this paper, we focus on the flux travel time distributions for discharge and evapotranspiration (termed reverse travel time distributions by *Botter et al.* [2011] and denoted p'_Q [T^{-1}] and p'_E [T^{-1}]), which describe the contributions of water with travel time T [T], to the discharge and evapotranspiration at time t [T].

[7] To conceptualize catchment-scale flow of water in relation to travel times of water, we consider the water balance of a catchment given by (following equation (3) in the work of *Botter et al.* [2011]):

$$\begin{aligned} &\frac{\partial s(T,t)}{\partial t}+\frac{\partial s(T,t)}{\partial T}=-q(T,t)-e(T,t) \\ &s(0,t)=J(t) \end{aligned}, \tag{1}$$

where $s(T, t)$ [L^3T^{-1}] is the storage with travel time T [T] at time t [T]; $q(T, t)$ [L^3T^{-2}] and $e(T, t)$ [L^3T^{-2}] are the discharge and evapotranspiration flux with travel time T at time t, and $J(t)$ [L^3T^{-1}] is the rainfall at time t. It is convenient to integrate equation (1) with respect to travel time T, which yields

$$s(T,t)=J(t-T)-\int_0^T q(\tau,t-T+\tau)\mathrm{d}\tau-\int_0^T e(\tau,t-T+\tau)\mathrm{d}\tau, \tag{2}$$

where τ [T] is an integration variable. Equation (2) has a clear physical meaning.

[8] 1. The first term $s(T, t)$ is the volume of water with travel time T that is stored inside the catchment at time t,

[9] 2. This water can only have entered the catchment by rainfall at time $t - T$: $J(t - T)$.

[10] 3. Water belonging to $s(T, t)$ cannot have left the catchment yet. Leaving may have occurred only via discharge and evapotranspiration for times between $t - T$ and t. We defined $q(T, t)$ and $e(T, t)$ as the fluxes of water with travel time T, leaving the catchment at time t. The last two terms of equation (2) thus give the volumes of water that entered via $J(t - T)$ and already left the catchment before time t by discharge and evapotranspiration, respectively.

[11] The resident travel time distribution, p_S [T^{-1}] and the flux travel time distributions for discharge, p_Q [T^{-1}], and evapotranspiration, p_E [T^{-1}] are defined by:

$$p_S(T,t) = \frac{s(T,t)}{S(t)}, \tag{3}$$

$$p_Q(T,t) = \frac{q(T,t)}{Q(t)}, \tag{4}$$

$$p_E(T,t) = \frac{e(T,t)}{E(t)}, \tag{5}$$

where $S(t)$ [L^3] is the total storage of water inside the catchment, $Q(t)$ [L^3T^{-1}] is the total discharge, and $E(t)$ [L^3T^{-1}] the total evapotranspiration at time t. These definitions are illustrated in Figure 1 and allow us to write equation (2) in terms of travel time distributions:

$$p_S(T,t)S(t) = J(t-T) - \int_0^T p_Q(\tau, t-T+\tau)Q(t-T+\tau)\mathrm{d}\tau - \int_0^T p_E(\tau, t-T+\tau)E(t-T+\tau)\mathrm{d}\tau. \tag{6}$$

[12] Equation (6) thus describes how resident and flux travel time distributions are related to each other and to storage, precipitation, discharge, and evapotranspiration. It is clear that the three travel time distributions are not independent and are not constant with time.

2.2. Transformation of Travel Times

[13] Travel time distributions that continuously change as function of time are not attractive "characteristic properties" of a catchment. Therefore, our aim was to find a transformation of travel time that could recast the problem of "how long have water parcels that leave a catchment, been inside this catchment?" (i.e., defining p_Q and p_E) into "what is the probability at time t that a water parcel inside a catchment leaves this catchment by discharge or evapotranspiration at time t?". The advantage of this different focus is that rather than considering past rainfall inputs, evapotranspiration fluxes, and discharges, we only need to consider the subsurface velocity field at time t. Hence, we may be able to define catchment specific probabilities of water leaving a catchment that are a function of the velocity field rather than past meteorological forcings. This recasting of the problem is achieved by a Smirnov transformation of travel time T [*Devroye*, 1986]:

$$g(T,t) \equiv \int_0^T p_S(\tau,t)d\tau, \tag{7}$$

where $g(T, t)$ is the cumulative probability of the resident travel time distribution for travel time T. This means that $g(T, t)$ has a value between 0 and 1, with 0 corresponding to the youngest and 1 to the oldest water inside a catchment. In a Lagrangian approach to water flow under stationary conditions, typically travel time is assumed to be a proxy for the position of a water parcel in a flow field. However, we argue that in a transient flow field the cumulative probability of resident travel time, in which all water parcels are sorted from young to old (0 to 1), is a better proxy (although still not perfect) for the position of a parcel than travel time itself. For example, were we able to freeze

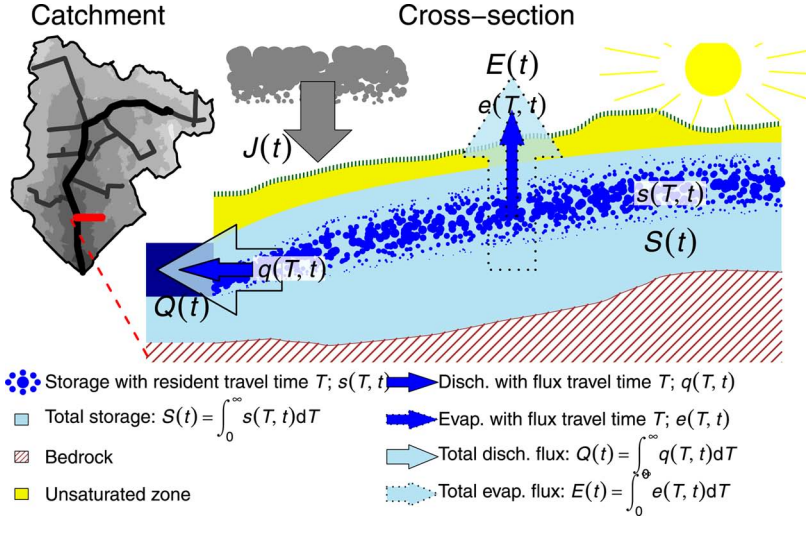

Figure 1. Schematic overview of fluxes and storage within a catchment.

a catchment instantaneously and thaw it again 200 days later, all water parcels inside the catchment would have aged 200 days, while both the cumulative probability of resident travel time for all parcels and the positions of all water parcels would be unchanged. Dry periods without rainfall cause a similar discrepancy between the evolution of travel time and the position of water parcels, which can partly be accounted for using the transformation of equation (7). This transformation also leads to new expressions for the flux travel time distributions (see Appendix A for a complete derivation). We denote this transformed travel time distribution by p^*:

$$p_Q^*(g,t) = \frac{p_Q(T(g,t),t)}{p_S(T(g,t),t)} = \frac{q(T(g,t),t)}{s(T(g,t),t)}\frac{S(t)}{Q(t)}, \tag{8}$$

$$p_E^*(g,t) = \frac{p_E(T(g,t),t)}{p_S(T(g,t),t)} = \frac{e(T(g,t),t)}{s(T(g,t),t)}\frac{S(t)}{E(t)}, \tag{9}$$

in which $T(g, t)$ is the travel time corresponding to a certain value of g as described by equation (7). This relation between T and g is not constant, but changes continuously, which explains its dependency on t. We call equations (8) and (9) Storage Outflow Probability (STOP) functions because they describe the rate at which storage with a certain travel time becomes discharge or evapotranspiration. Effectively, STOP functions describe the probability at time t of a stored water parcel to become discharge or evapotranspiration at time t, relative to the average probability of all particles to become discharge $\left(\frac{Q(t)}{S(t)}\right)$ or evapotranspiration $\left(\frac{E(t)}{S(t)}\right)$. From a discharge and evapotranspiration perspective this is equal to describing catchment-scale mixing. We emphasize that these STOP functions strongly resemble the Age functions described by *Botter et al.* [2011], but our reasoning that lead to the derivation of STOP functions is quite different. The Age functions, proposed by *Botter et al.* [2011], are given by:

$$\omega_Q(T,t) = \frac{p_Q(T,t)}{p_S(T,t)}, \tag{10}$$

$$\omega_E(T,t) = \frac{p_E(T,t)}{p_S(T,t)}. \tag{11}$$

[14] The only difference between STOP functions and Age functions is the transformation of T into g. The advantages of this transformation, however, are threefold. First, we expect the relation between STOP functions and the flow field to be more constant in time than the relation between flow field and Age functions for reasons explained before. This implies that STOP functions can be parameterized more effectively by a constant function or a constant relation between storage and STOP functions. This hypothesis will be tested later in this paper. Second, because STOP functions are transformed travel time distributions, they are by definition probability density functions (PDF) describing the probability of a water parcel inside a catchment at time t, to become discharge or evapotranspiration at time t, relative to the average probability of water leaving a catchment at time t. Age functions also describe the ratio between storage with travel time T and water leaving a catchment with travel time T, but are not PDFs because they do not necessarily integrate to 1. We can thus use the large array of existing PDFs to parameterize STOP functions. Third, rescaling the travel time domain into the g domain allows us to compare mixing behavior of catchments independent of their absolute travel time. This means that catchments that have completely different absolute travel times may have similar subsurface mixing behavior, which now can be formalized by similar STOP functions. STOP functions thus isolate the mixing process from travel time distributions and therefore have a clearer physical meaning then Age Functions.

2.3. Shape of STOP Functions

[15] For an intuitive understanding of STOP functions, several limiting cases are helpful (the first two are also briefly discussed by *Botter et al.* [2011]).

[16] 1. Perfectly mixed reservoir: water that leaves the catchment is a perfectly mixed subsample of storage and thus the flux travel time distribution is equal to the resident travel time distribution. This means that all water within the catchment is drained at the same rate resulting in a STOP function with value 1.

[17] 2. Piston flow ("First in first out"): water is pushed through the system without any mixing. The oldest water is the first water to leave the catchment. The corresponding STOP function is a Dirac-distribution at $g = 1$.

[18] 3. "Last water in is first water out": This results in a STOP function that is a Dirac-distribution at $g = 0$ with the youngest water leaving the catchment first.

[19] These three idealized flow systems encompass realistic flow fields and thus provide us with valuable benchmarks for interpreting STOP functions of more complex flow systems. Additional understanding of the shape of the STOP functions for different types of landscapes is obtained by numerically solving STOP functions for three relatively simple two-dimensional transects (Figure 2), with steady state and horizontal (Dupuit assumption) groundwater flow. In Appendix B analytical expressions for resident and flux travel time distributions, Age functions and STOP functions of such two-dimensional transects are presented. For Figure 2, we numerically solved the position of the water table for three rainfall intensities and three bedrock shapes (i.e., solving equation (B1)). From these water tables, we calculated the resident and flux travel time distribution, the discharge Age function and the discharge STOP function according to the corresponding equations in Appendix B.

[20] In Figure 2, transect A (Figure 2a) resembles a lowland agricultural field with a flat bedrock or impermeable layer. Transect B (Figure 2b) represents an idealized hillslope (4% slope) in an undulating landscape, and transect C (Figure 2c) is a more realistic hillslope with an irregularly shaped bedrock. The second row of panels in Figure 2 shows that each transect has a resident travel time distribution that is distinctly different from the flux travel time distribution. This means that these transects cannot be considered to be perfectly mixed, which would yield equal resident and flux travel time distributions, and thus these simple examples illustrate the necessity to formulate a more general parameterization for subsurface mixing. In

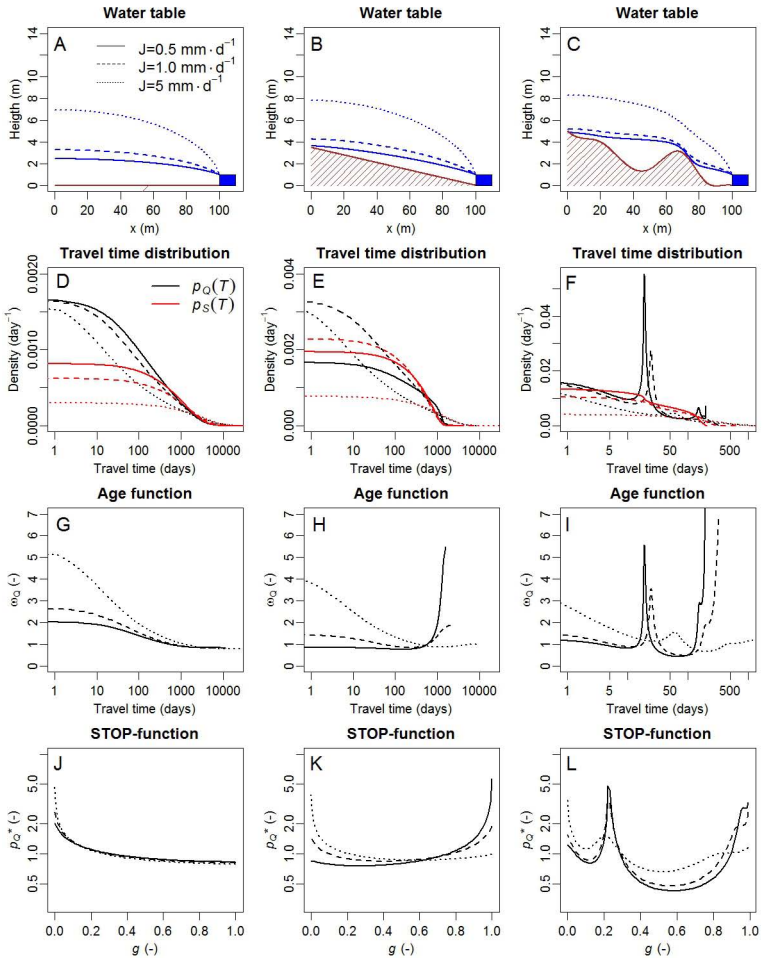

Figure 2. Water tables, resident and flux travel time distributions, Age functions and the STOP-functions for three transects with different bedrock forms (brown line and brown striped area) and three rainfall intensities (J). In the graphs of the STOP-function, a g-value of 0 corresponds to the youngest water inside the catchment, whereas a g-value of 1 corresponds to the oldest water inside the catchment.

the 3rd and 4th row of Figure 2, we show both the Age functions and STOP functions for each transect.

[21] For the flat agricultural field (transect A) the resident and flux travel time distributions show that the contribution of young water to discharge is significantly larger than the contribution of young water to storage. Lowland landscapes thus have a preference for discharging the younger water from the storage. This result is shown more clearly by the Age functions and STOP functions in Figures 2g and 2i, respectively. Especially the STOP functions show that the relative discharge rate of the youngest water ($g = 0$) is far larger than the relative discharge rate of the oldest water in the catchment ($g = 1$). Here the strength of the interpretation provided by the STOP function is apparent: it directly shows which water stored within the catchment is dominating discharge. The three rainfall intensity scenarios for bedrock A demonstrate that, although the travel time distributions and Age functions between the scenarios differ significantly (Figures 2d and 2g), the shape of the STOP function is hardly affected by precipitation intensity (Figure 2j). Scaling travel time via equation (7), which reshapes the Age function into the STOP function, thus greatly improves the comparability of subsurface mixing between these scenarios and demonstrates the suitability of the STOP function as a catchment characteristic.

[22] For the sloped bedrock form B, we see a clear shift in discharge behavior with precipitation intensity. For short travel times and low rainfall intensity the resident travel time distribution exceeds the flux travel time distribution, while for the high rainfall intensity the flux travel time distribution exceeds the resident travel time distribution. This means that this hillslope has a preference for discharging old water under low precipitation and storage conditions and a preference for discharging young water under high precipitation and storage conditions. This is again most clearly illustrated by the STOP functions (Figure 2k). It appears that hillslopes where groundwater level gradients are not affected by the slope of the bedrock, preferentially discharge relatively young water in agreement with the results of transect A. Catchments where the bedrock slope dominates groundwater level gradients, though, preferentially discharge relatively old water. This difference regarding whether or not bedrock affects groundwater flow has also been recognized by *Berne et al.* [2005] and *Harman and Sivapalan* [2009] who distinguished hillslope groundwater flow as being advective (the effect of bedrock gradient) and

diffusive (part of groundwater level gradient not explained by bedrock). The Péclet number for hillslopes of *Berne et al.* [2005] that characterizes the relative importance of diffusive versus advective flow could be a useful tool to help understand the shape of the STOP function for hillslopes in future studies.

[23] If we compare the Age function and the STOP function for transect B, it is apparent that the STOP functions and the differences between STOP functions are easier to parameterize than the Age functions for the different precipitation intensities. It is also clear that the mixing process of example hillslope B needs to be described with a STOP function that is a function of storage and cannot be described with a single STOP function covering all hydrological conditions.

[24] Bedrock form C illustrates the effect of irregularly shaped bedrock on resident and flux travel time distributions. The curved shape of the bedrock causes local acceleration of the groundwater flow. Areas with relatively large groundwater flow velocities contribute strongly to the flux travel time distribution, which results in the spike of the flux travel time distribution of transect C (i.e., a relatively large groundwater flow velocity means a relatively small spatial gradient in travel time (dT/dx). This in turn implies a large area with similar travel times and thus a large volume of rainfall with similar travel times, which creates a spike in the travel time distribution). Because the contrast in groundwater flow velocities decreases with increasing rainfall, the spikes in the flux travel time distribution, Age functions and the STOP functions reduce for larger rainfall intensities. Again, for this hillslope a single fit of the STOP function will not suffice to describe subsurface mixing under all hydrological conditions. More research on the upscaling behavior of STOP functions to entire catchments with many of such hillslopes is needed to understand the potential of the STOP functions in hilly catchments.

[25] From Figure 2, we conclude that STOP functions effectively describe the preference for discharging relatively old or young water and thus effectively describe the mixing process occurring in the subsurface of a catchment. However, only if groundwater head gradients increase proportionally with increasing storage (equation (B9)), the STOP function is relatively independent of the amount of storage. This generally seems to be the case for our flat examples but not for our hillslope examples.

2.4. STOP Functions for a Lowland Catchment

[26] Another way to learn more about the shape of STOP functions for a real catchment is via detailed transient particle tracking simulations that allow us to quantify the dynamics of the three travel time distributions (storage, discharge and evapotranspiration). In the work of *Van der Velde et al.* [2009, 2010a] such a particle tracking simulation was introduced for the Hupsel Brook catchment (6.5 km^2) in the Netherlands. *Van der Velde et al.* [2009] constructed a groundwater model for this catchment that simulates groundwater flow with a 5x5 m spatial resolution on a daily basis for the period 1983–2008. This model was extended with transient particle tracking by *Van der Velde et al.* [2010a] to quantify dynamics in the resident and flux travel time distributions for discharge and evapotranspiration. In this study, we use those simulations to calculate both Age functions and STOP functions for the Hupsel Brook catchment. For each model time step Age functions for discharge and evapotranspiration were calculated by dividing the flux travel time distribution by the resident travel time distribution according to equations (10) and (11). Subsequently, the Age functions were converted to STOP functions by transforming travel time into g for each model time step using equation (7). We grouped the Age functions and STOP functions for average, wet and dry storage conditions, to investigate the effect of the flow field on the shape of both functions (Figure 3).

[27] A comparison of the temporal variability (light gray areas in Figure 3) of STOP functions and Age functions for discharge reveals that the STOP function of discharge is significantly more constant than the Age function. Also, the shape of STOP functions is easier to parameterize than that of Age functions. For these reasons, we consider STOP functions better suited to describe catchment-scale mixing in the Hupsel Brook catchment. Figure 3c shows an even stronger preference of this catchment to discharge young water than the results of the steady state transect analyses of Figure 2 already suggested. We attribute this strong preference for discharging young water to fast flow routes such as drainage and overland flow that were accounted for in the groundwater model simulations but not in the simulations of Figure 2.

[28] Another remarkable result from Figure 3c are the small differences between STOP functions when storage volumes change, in spite of the major changes in the flow field through the seasons: from regional flow paths under dry conditions to local and shallow flow paths under wet conditions [*Van der Velde et al.*, 2009]. Apparently, this does not strongly affect mixing behavior of this catchment.

[29] The STOP functions for discharge (Figure 3c) and evapotranspiration (Figure 3d) are quite different. This difference is a fundamental property that "fingerprints" catchments (see also the partitioning of water within catchments described by *Brooks et al.* [2010]). Comparing STOP functions for discharge and evapotranspiration, we see that evapotranspiration has an even stronger preference for the youngest water within the storage. The evapotranspiration flux approaches a "last in first out" system, with very low probabilities of removing the older water from the storage. This observation shows clearly that catchment travel times need to be characterized by separate STOP functions for discharge and evapotranspiration. The STOP functions for evapotranspiration seem to vary more as a function of storage than those for discharge, but this can also be partly attributed to relatively large uncertainties in the particle tracking algorithm for evapotranspiration, especially under dry conditions.

[30] In view of the shape of the STOP functions in Figures 2 and 3 and those of the limiting cases discussed (beginning of section 2.3), which all show a preference for young ($g = 0$) or old water ($g = 1$) and integrate to 1 for g values between 0 and 1, we propose to approximate the STOP function with a Beta distribution. The Beta distribution has two parameters, a and b. When both parameters have value 1 the Beta distribution reduces to a uniform distribution with a density of 1 for all g values between 0 and 1, thus giving a parameterization for complete mixing. Values for a smaller than 1 indicate a preference for discharging young water,

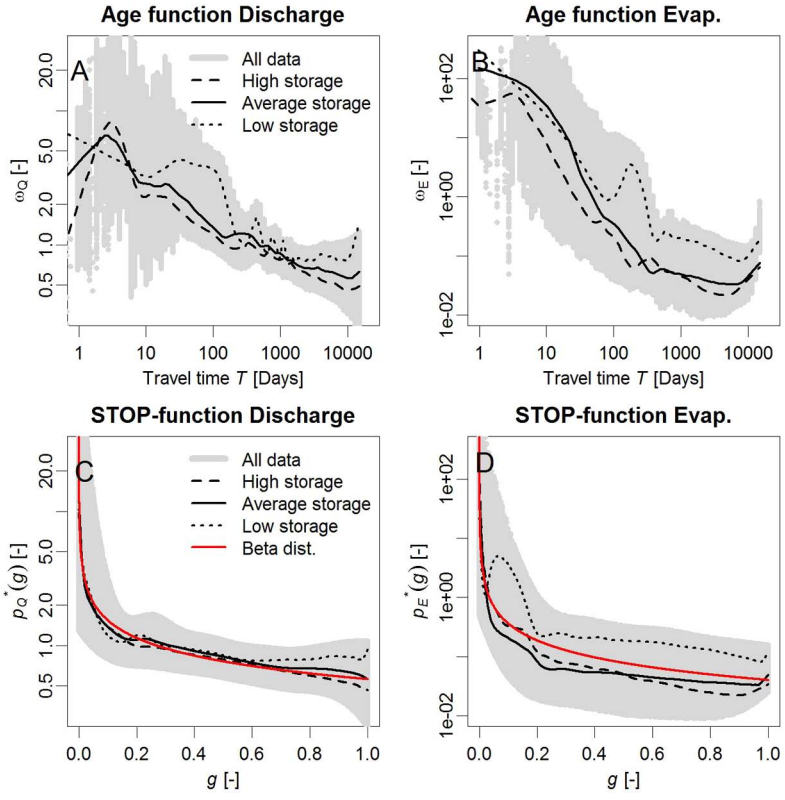

Figure 3. Age functions and STOP-functions derived from particle tracking simulations of the Hupsel Brook catchment. The gray points indicate the temporal variability of Age functions and STOP-functions. The high storage conditions correspond to the fifth percentile largest daily storage volumes. The average storage conditions correspond to the 45th to 55th percentile of daily storage volumes, and the low storage conditions correspond to the fifth percentile lowest daily storages. The red line is a fit of the beta distribution to the STOP-functions corresponding to average storage conditions. Note the different vertical axes for the discharge and evapotranspiration graphs.

while b values smaller than one indicate a preference for old water. The Beta distribution can fit the shape of the STOP functions for the limiting cases, hillslopes A and B from Figure 2 and the STOP functions derived from the particle tracking for the Hupsel Brook catchment (Figure 3). Fits of the Beta distribution are added in Figure 3: an a value of 0.6 and a b value of 1 for discharge and an a value of 0.03 and a b value of 1 for Evapotranspiration. In section 3, we will apply these values to explore the connections between the STOP function and travel time distributions.

3. STOP Function Applications

3.1. Transient Travel Time Distributions and Stream Water Concentration

[31] In section 2, we have derived a realistic parameterization of the discharge and evapotranspiration STOP functions for the Hupsel Brook catchment from a spatially distributed groundwater model. Because of the long computation times of the groundwater model and its many parameters, the groundwater model itself is not suited to explore parameter sensitivity on travel time distributions and stream water concentrations. Moreover, the groundwater model is constrained by its Darcian groundwater flow approximation and thus excludes preferential flow processes, which are likely to be very important in quantifying travel time distributions [*Beven*, 2010]. The STOP functions derived from the groundwater model can, however, be used as a first approximation that accounts for the mixing caused by topography and subsurface permeability in simple catchment-scale water balance approaches. Such water balance models can more accurately calculate fluxes (including preferential flow) and combined with STOP functions, these models can calculate time-varying flux travel time distributions and concentrations with higher temporal resolutions than the groundwater model and for many more parameter combinations. If tracer concentration measurements indicate that preferential flow is important and a larger preference for young water is evident from measurements, the parameters of the STOP functions can be adjusted to account for the mixing effect caused by preferential flow processes. This last step, however, is not performed in this study. Our approach is summarized in 3 steps.

[32] 1. We used modeled hourly time series of storage, discharge and evapotranspiration derived with the catchment-scale water balance model described in the work of *Van der Velde et al.* [2011]. They defined 500 parameter sets that described observed discharges of the Hupsel Brook equally well. We used all 500 parameter combinations, which has the benefit that we directly obtain an

indication of the travel time uncertainties originating from water balance uncertainties.

[33] 2. For each time step and each parameter set, we numerically solved equations (3)–(9), as we were unaware of the analytical solutions derived by *Botter et al.* [2011] at that time. Obviously, our numerical and *Botter et al.* [2011] analytical approach should yield similar results, but this was not tested. The numerical approach yielded 500 time series of flux travel time distributions for discharge and evapotranspiration. The STOP functions p_Q^* and p_E^* were derived from particle tracking simulations for the Hupsel brook catchment as explained in the previous paragraph.

[34] 3. Based on the discharge flux travel time distributions of step 2, we calculated concentrations of a fictive solute that undergoes the same processes as nitrate, i.e., diffusion and degradation. This relative concentration, $\overline{C}(t)$, which has a value between 0 and 1, is calculated by a convolution of temporally varying travel time distributions with a constant relation between travel time and concentration. This is the simplest way of relating travel time distributions to stream concentrations for solutes that do not enter a catchment by rainfall:

$$\overline{C}(t) = \int_0^\infty p_Q(T,t)(1 - e^{-r_d T})e^{-r_n T}\mathrm{d}T. \tag{12}$$

[35] The constant relation between travel time and relative concentration is given by $(1 - e^{-r_d T})e^{-r_n T}$, which can be interpreted as follows: a water parcel with zero concentration falls as rainfall on a catchment. Along its travel path inside the catchment, this water parcel is likely to receive some nitrate by diffusion from other parcels that have been in the catchment longer and already have higher nitrate concentrations. The catchment-scale average rate of receiving nitrate by diffusion as a function of the concentration difference between the water parcel and water parcels in its surroundings is described by r_d [T^{-1}]. If this water parcel continuous to travel inside the catchment, the chance that it encounters an anoxic zone where nitrate denitrifies into nitrogen gas increases. The catchment-scale average rate of this degradation as a function of travel time is described by r_n [T^{-1}]. A concentration of 1 is never reached and can be interpreted as the average concentration water parcels have on locations that need zero travel time for a new water parcel to reach. However, on these locations new water parcels need diffusion time to equilibrate with their surroundings, thus never reaching a concentration of 1 (i.e., water parcels fall on locations with potentially high nitrate concentrations, but due to overland flow and preferential flow paths do not spend enough time in contact with the soil to take up much nitrate). Of course this constant relation between travel time and concentration is a huge simplification of all processes and spatial and temporal dynamics herein. It should be regarded as a pragmatic approach that allows us to isolate the effects of temporal variability in travel time distributions on stream concentrations. This works well for short periods during which the total amount of nitrate in the catchment and its spatial distribution do not change significantly. More details on the underlying assumptions of a constant travel time concentration relation can be found in the work of *Van der Velde et al.* [2010a]. Example values for r_d and r_n for nitrate are adopted from the results of *Van der Velde et al.* [2010a]: $r_d = 0.2\ \mathrm{d}^{-1}$, $r_n = 0.0025\ \mathrm{d}^{-1}$.

[36] Figure 4b shows the calculated resident and flux travel time distributions at four moments during a storm event in March 2008 (Figure 4a). The contribution of this particular storm event to the resident (p_S) and flux travel time distributions (p_Q) is indicated in light blue (Figure 4b). From the distributions in Figure 4b, we conclude that this storm event mainly contributed to discharge (p_Q) and only little to storage (p_S): at the end of the storm event, the contribution of water from this storm event (in light blue) to the catchment storage (p_S) is small. The catchment was already wet at the onset of the storm, which resulted in a discharge flux that was almost equal to the precipitation input. The discharge STOP function describes a preference for discharging the younger water from the storage, resulting in a relatively large contribution of event water to the discharge following the rainfall. This is typical for a lowland catchment under wet conditions with large contributions of overland flow [*Van der Velde et al.*, 2010b].

[37] However, had the same event occurred following a relatively dry period with low groundwater tables, rainfall predominantly would have been stored in the catchment instead of producing a high discharge [*Brauer et al.*, 2011]. In that case, rain would have contributed far more to the resident travel time distribution, as can be seen from previous rain events that indeed contributed substantially to the overall storage and remained to do so for a long period (spikes in p_S shown in Figure 4b). The type of mixing thus controls that storage in this lowland catchment mainly consists of water from rainfall events that occurred after dry periods (large summer storms or the first rainfall events in autumn). Recognizing that antecedent conditions control the fate of rain water, Figure 4 nicely illustrates the versatility of our approach to derive time-varying travel time distributions, by combining rainfall, evapotranspiration, storage and discharge with a subsurface mixing scheme that is determined by landscape and vegetation properties.

[38] The calculated relative concentration and measured nitrate concentrations during the storm event of March 2008 are shown in Figure 4c and this period is extended in Figure 5. The dynamics in observed nitrate concentration is adequately reproduced by the calculated relative concentration. Although only the dynamics of modeled relative concentration and measured nitrate concentration can be compared, the potential of describing water quality dynamics with relatively simple travel time-based models is evident. Vice versa, Figure 5 also shows that event-based surface water quality records contain a wealth of information on flow routes and mixing processes inside a catchment and it seems feasible to infer the shape of the STOP functions directly from time series of tracers. Conservative tracers that enter a catchment by rainfall seem especially suited for such analysis [*Kirchner et al.*, 2003; *Lyon et al.*, 2008; *McGuire et al.*, 2005]. Hydrological research has only scratched the surface of inferring subsurface information from water quality records with a high temporal resolution. It is clear that combining hydrological water balance models with travel time approaches such as the STOP functions can greatly improve our understanding of hydrological pathways within catchments and thus advance our predictive capabilities of solute spreading within catchments.

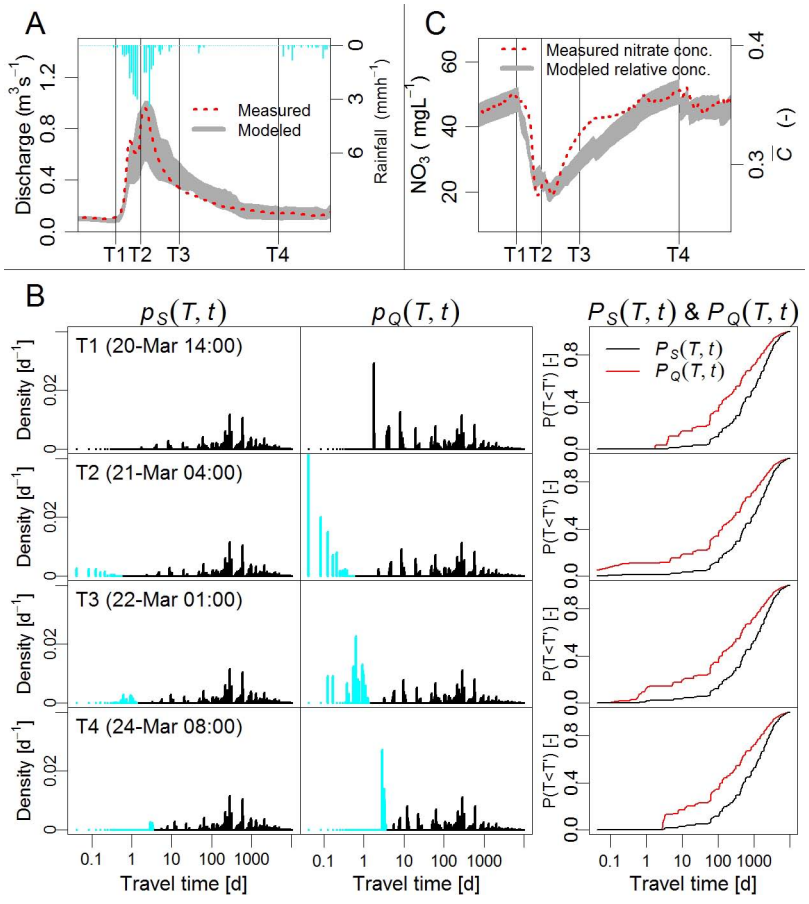

Figure 4. (a) The discharge peak of the Hupsel Brook following a rainfall event in March 2008. The gray band indicates the results of 500 parameter sets all describing measured discharge equally well [*Van der Velde et al.*, 2011]. (b) The calculated resident travel time distributions (p_S), flux travel time distributions of discharge, p_Q, and their cumulative distributions, p_S and p_Q for a single parameter set. The blue colors indicate the contribution of water from this storm event to the travel time distribution. (c) The observed nitrate concentration at the catchment outlet is shown together with the calculated relative concentration, $\overline{C}$. The gray band indicates the results of all 500 parameter combinations. Note that the*y* axis of the cumulative resident time distribution (p_S) equals *g*.

3.2. Relations Between STOP Functions, Landscape and Average Travel Time Distributions

[39] The effects of discharge and evapotranspiration STOP functions on the travel time distribution of discharge are explored by calculating long term (1983–2010) average travel time distributions for four different combinations of STOP functions.

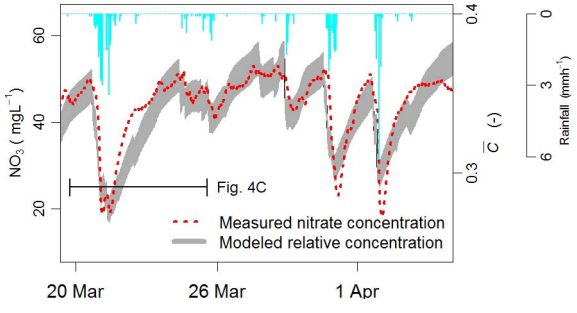

Figure 5. Extended version of Figure 4c, with additional rain events following the rain event of Figure 4c.

[40] 1. Mixing according to the Hupsel Brook catchment, the STOP functions derived from Figure 3.

[41] 2. Evapotranspiration from a perfectly mixed reservoir, discharge STOP function from Figure 3.

[42] 3. Discharge from a perfectly mixed reservoir, evapotranspiration STOP function from Figure 3.

[43] 4. Discharge from a reservoir with mixing as could occur in a sloping catchment based on results from Figure 2 and the evapotranspiration STOP function from Figure 3.

[44] For each of these STOP function combinations we calculated flux travel time distributions for discharge following the procedure as described in section 3.1. From these time series of flux travel time distributions we calculated the temporally averaged flux travel time distribution over the entire period. Figure 6a shows that changing the subsurface mixing scheme for discharge from a preference for young water (mixing according to the Hupsel Brook catchment) to a perfectly mixed reservoir, or mixing as could occur in a

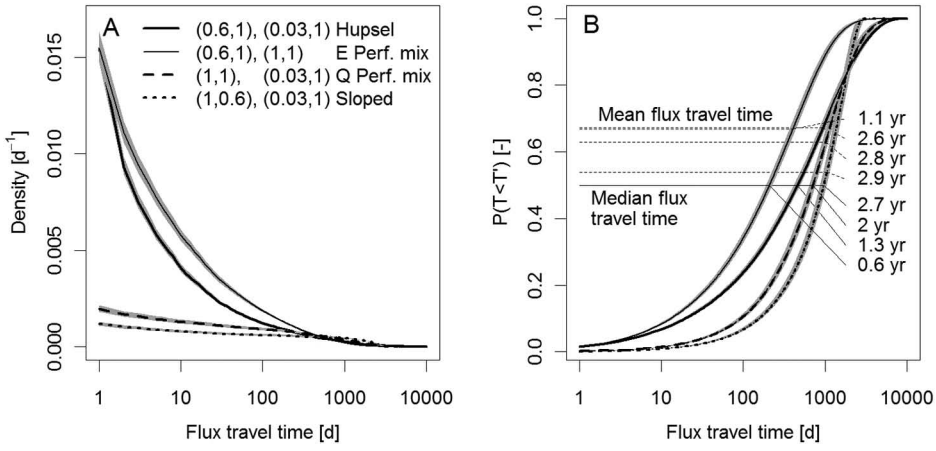

Figure 6. The effect of catchment subsurface mixing schemes for (a) discharge and evapotranspiration on average flux travel time distributions for discharge and (b) cumulative travel time distributions for discharge. The legend shows four numbers for each mixing scheme: the first 2 numbers correspond to the *a* and *b* of the discharge STOP-function, the second set of 2 numbers corresponds to the a and b values of the evapotranspiration STOP-function. The gray bands indicate the uncertainty stemming from the 500 different parameter sets describing the hydrology (see also Figure 4).

sloping catchment, greatly decreases the contribution of water with travel times less than a 100 days to its discharge. Exactly the contributions of these relatively short travel times affect overall solute concentrations most, because during these short travel times the concentration differences between different types of water inside a catchment are largest. This partly explains the observed large dynamics in stream concentrations of lowland catchments [*Tiemeyer et al.*, 2008; *Rozemeijer et al.*, 2010] compared to surprisingly constant stream concentrations observed in many sloping catchments [e.g., *Kirchner*, 2003].

[45] From Figure 6 we see that changing the subsurface mixing scheme of evapotranspiration strongly affects the travel time distribution of discharge as well. As grass and maize are the dominant types of vegetation in the Hupsel Brook catchment, it is reasonable to assume that the relatively short roots predominantly extract the younger water from the overall storage. Deep roots of trees on shallow soils, on the other hand, may extract a much more mixed subsample of storage. Figure 6b shows that the perfectly mixed assumption for evapotranspiration would decrease the mean flux travel time of stream water in the Hupsel Brook discharge from 2.6 to 1.1 year. This result demonstrates that a correct subsurface mixing scheme (STOP function) for evapotranspiration is just as important as the subsurface mixing scheme of discharge, even if we are only interested in the travel times of discharge. Also, it shows the large effect vegetation can have on discharge travel times and thus on solute concentrations in streams, even when the amount of evapotranspiration stays the same.

[46] Furthermore, Figure 6b shows that the overall shape of the discharge travel time distribution is strongly related to the mixing scheme for discharge. A preference for discharging old water yields a much narrower cumulative distribution than a preference for young water. The mean of the travel time distribution, however, is hardly affected by the type of subsurface mixing for discharge: the effect of a discharge volume increase of young water on the mean travel time is countered by increasing travel times of the oldest water (i.e., the oldest water becomes older). This result implies that the mean travel time of a catchment contains very little information on the type of subsurface mixing.

[47] Although assuming a constant STOP function is a much weaker assumption than assuming a constant travel time distribution or a constant Age function to characterize subsurface flow in a catchment, still, it is likely that in many catchments the STOP function will change with storage or subsurface flow patterns (as shown for the hillslopes in Figure 2). Therefore, more research is needed to understand the behavior of STOP functions with changing flow patterns and to understand the relation between STOP functions and landscape and vegetation properties. If it proves feasible to parameterize the STOP function based on landscape characteristics, the STOP function may become an indispensable tool for solute transport modeling in data-poor regions, because of its small number of parameters and its flexible and intuitive use in combination with a water balance approach.

4. Conclusions

[48] In this paper, we introduce a new transformation of travel times. The transformed travel time distributions we call Storage Outflow Probability (STOP) functions. The advantage of STOP functions over the commonly used travel time distribution is that STOP functions are continuous functions which are relatively constant in time, or only a function of the flow velocity field. This is in contrast to travel time distributions which change continuously with rainfall and evapotranspiration and are discontinuous due to the discontinuous nature of rainfall. Effectively, STOP functions quantify the probability of water parcels in storage to leave a catchment by discharge or evapotranspiration. This is equal to quantifying the degree of catchment-scale mixing. We showed that by combining STOP functions with a water balance approach, it is possible to calculate temporal variability

of travel time distributions, and describe contrasting flux travel time distributions for discharge, evapotranspiration and other flow routes leaving the catchment. This last property of STOP functions is essential for describing realistic travel times of water within catchments, which is demonstrated by the sensitivity of the long term average travel time distribution of discharge to both discharge and evapotranspiration STOP functions. STOP functions can serve as a new catchment characteristic, fingerprinting the degree of subsurface mixing and catchment travel time distribution dynamics and catchment vulnerability to pollution spreading.

[49] Recently *Botter et al.* [2011] introduced Age functions, which are similar to our STOP functions. However, the STOP function approach has several important advantages: STOP functions were found to be more constant in time than Age functions for our lowland catchment; STOP functions are probability density functions and can thus be parameterized by existing PDFs; and STOP functions isolate mixing behavior from the travel time distribution, and thus have a clearer physical meaning. This enables the comparison of the mixing behavior between catchments.

[50] We showed that the Hupsel Brook lowland catchment exhibits strongly incomplete mixing with a preference for discharging young water. Hillslopes, on the other hand, may have a preference for old water under dry conditions and young water under wet conditions as was shown by a theoretical example. This demonstrates that stream water travel time distributions can be calculated only with an appropriate parameterization of subsurface mixing corresponding to the landscape and vegetation characteristics of a catchment. The STOP functions described in this paper provide a method to do so. Some caution is appropriate regarding the general applicability of STOP functions in sloping catchments. The examples in Figure 2 suggest that in sloping catchments a strong relation can exist between storage and the STOP function. For such catchments it may prove necessary to derive relations between storage and the degree of mixing. This, of course, complicates the use of STOP functions and diminishes the advantage of only requiring two parameters to describe each flow route. More research in this direction is needed.

[51] A practical application of STOP functions, demonstrated in this paper, is to derive the shape of the STOP functions from spatially distributed particle tracking simulations. Such a compact and simple summary of a complex transient numerical model has the huge advantage of being able to include all the available information on topography and subsurface into the complex model and derive from its results the catchment-scale behavior of mixing and flow-path dynamics, i.e., STOP functions [see also *Van der Velde et al.*, 2009]. A simple water balance model, combined with STOP functions for each flow route derived from the complex model allows for parameter optimization within bounds set by the complex model and calculation of uncertainty bounds for travel times and solute transport. Such results are often impossible to obtain from the spatially distributed numerical simulations because of the many parameters involved, the long calculation times and the conceptual constraints underlying the spatially distributed model, for example with respect to preferential flow.

[52] In our opinion, the way forward is to (re)analyze time series of tracer composition in precipitation and streamflow around the world and identify typical subsurface mixing behaviors for both discharge and evapotranspiration. Especially, time series of tracer composition with high temporal resolutions, as demonstrated in Figure 5, contain valuable information about the flow routes and mixing processes inside a catchment, which still are a major source of uncertainty in current hydrological models. Identifying mixing behavior for discharge as a function of landscape and drainage network and for evapotranspiration as a function of vegetation type and soil properties poses a major challenge for future hydrological research. Once these relations are understood, application of STOP functions to data-poorer regions will become possible.

Appendix A

[53] The transformation of travel time T into g via equation (7) also yields transformed flux and resident travel time distributions. First, we focus on the transformed flux travel time distribution of discharge, p_Q^*, which obeys:

$$p_Q(T,t)\mathrm{d}T = p_Q^*(g(T,t),t)\mathrm{d}g. \tag{A1}$$

[54] This equation can be rewritten into:

$$p_Q^*(g(T,t),t) = p_Q(T,t)\left|\frac{\mathrm{d}T}{\mathrm{d}g}\right|. \tag{A2}$$

[55] From equation (7) it follows that:

$$\frac{\mathrm{d}T}{\mathrm{d}g} = \frac{1}{p_S(T,t)}. \tag{A3}$$

[56] Combining equations (A2) and (A3) leads to the expression

$$p_Q^*(g,t) = \frac{p_Q(T(g,t),t)}{p_S(T(g,t),t)}. \tag{A4}$$

[57] We call this equation the discharge Storage Outflow Probability (STOP) function. Similarly, we can define a transformed travel time distribution for evapotranspiration and a transformed resident travel time distribution:

$$p_E^*(g,t) = \frac{p_E(T(g,t),t)}{p_S(T(g,t),t)}, \tag{A5}$$

$$p_S^*(g) = 1. \tag{A6}$$

[58] The above derivation of STOP functions shows that they are by definition probability density functions, which is one of the major advantages of STOP functions over Age functions [*Botter et al.*, 2011].

Appendix B

[59] The water table for a two-dimensional cross section with no water storage in the unsaturated zone, and stationary rainfall is described by the following differential equation:

$$Jx = -k(H(x) - B(x))\frac{\mathrm{d}H}{\mathrm{d}x}. \tag{B1}$$

where J [LT^{-1}] is rainfall, k [LT^{-1}] is the hydraulic conductivity of the soil, $H(x)$ [L] the height of the water table at location x [L] and $B(x)$ [L] the height of the impermeable bedrock. All examples in Figure 2 have a hypothetical hillslope/field length, L [L], of 100 m, a hydraulic conductivity, k, of 1 m d^{-1}, boundary conditions $H(100) = 1$, $B(100) = 0$ and zero lateral flux at $x = 0$ (see Figure 2 for the setup of 3 examples using these boundary conditions).

[60] Given a Dupuit assumption for groundwater flow (only horizontal flow), the velocity of groundwater, V [LT^{-1}], as function of location x is given by:

$$V(x) = \frac{J\,x}{n(H(x) - B(x))}, \tag{B2}$$

with n [-] the soil porosity. From this velocity field we can calculate the flux travel time belonging to location x by:

$$T(x) = \int_x^L \frac{1}{V(x)}\,\mathrm{d}x. \tag{B3}$$

[61] This function can be numerically inverted to give the location as function of travel time, $x(T)$. Unfortunately, no easy analytical expression exists for $x(T)$, even for basic examples. The function $x(T)$ allows us to find an expression for the storage with travel time T, $s(T)$ [L^2T^{-2}]. This storage is found by the volume of rainfall on locations that need more time to reach the outlet than travel time T:

$$s(T) = x(T)J. \tag{B4}$$

[62] The discharge, $q(T)$ [LT^{-2}], with travel time T is given by:

$$q(T) = -J\frac{\mathrm{d}x}{\mathrm{d}T} = J\,V\Big(x(T)\Big) \tag{B5}$$

with $\dfrac{dx}{dT} = -V(x)$ derived from equations (B3). The flux and resident travel time distributions of stationary two-dimensional flow problems, with only horizontal flow, can now be written as:

$$p_Q(T) = \frac{q(T)}{Q} = \frac{V(x(T))}{L}, \tag{B6}$$

$$p_S(T) = \frac{s(T)}{S} = \frac{x(T)J}{n\displaystyle\int_0^L \Big(H(x) - B(x)\Big)\mathrm{d}x}, \tag{B7}$$

where Q [LT^{-1}] and S [L^2] are the total discharge (which for stationary examples is equal to the rainfall, J) and the total storage, respectively. These travel time distributions lead directly to an expression for the Age function

$$\omega_Q(T) = \frac{p_Q(T)}{p_S(T)} = \frac{\frac{1}{L}\displaystyle\int_0^L (H(x) - B(x))\mathrm{d}x}{H(x(T)) - B(x(T))}. \tag{B8}$$

[63] The STOP function is obtained by transforming T into g (see equation (7))

$$p_Q^*(g) = \frac{\frac{1}{L}\displaystyle\int_0^L (H(x) - B(x))\mathrm{d}x}{H(x(T(g))) - B(x(T(g)))}. \tag{B9}$$

[64] **Acknowledgments.** The comments of three anonymous reviewers greatly helped to improve our manuscript. We also thank G.A. Destouni for providing several valuable suggestions. Support for this work was received from Stockholm University's Strategic Marine Environmental Research Funds through the BEAM Program. S.E.A.T.M. van der Zee appreciates support by the International Network NUPUS, funded by DFG (Germany) and NWO (Netherlands), EU project SoilCAM (ENV.2007.3.1.2.2 grant agreement 212,663) and discussions with Andrea Rinaldo (EPFL, CH).

References

Berne, A., R. Uijlenhoet, and P. A. Troch (2005), Similarity analysis of subsurface flow response of hillslopes with complex geometry, *Water Resour. Res.*, *41*, W09410, doi:10.1029/2004WR003629.

Beven, K. J. (2010), Preface: Preferential flows and travel time distributions: Defining adequate hypothesis tests for hydrological process models, *Hydrol. Processes*, *24*, 1537–1547.

Bloem, E., J. Vanderborght, and G. H. de Rooij (2008), Leaching surfaces to characterize transport in a heterogeneous aquifer: Comparison between flux concentrations, resident concentrations, and flux concentrations estimated from temporal moment analysis, *Water Resour. Res.*, *44*, W10412, doi:10.1029/2007WR006425.

Botter, G., E. Bertuzzo, and A. Rinaldo (2010), Transport in the hydrologic response: Travel time distributions, soil moisture dynamics, and the old water paradox, *Water Resour. Res.*, *46*, W03514, doi:10.1029/2009WR008371.

Botter, G., E. Bertuzzo, and A. Rinaldo (2011), Catchment residence and travel time distributions: The master equation, *Geophys. Res. Lett.*, *8*, L11403, doi:10.1029/2011GL047666.

Brauer, C. C., A. J. Teuling, A. Overeem, Y. van der Velde, P. Hazenberg, P. M. M. Warmerdam, and R. Uijlenhoet (2011), Anatomy of extraordinary rainfall and flash flood in a Dutch lowland catchment, *Hydrol. Earth Syst. Sci.*, *15*, 1991–2005.

Brooks, R. J., H. R. Barnard, R. Coulombe, and J. J. McDonnell (2010), Ecohydrologic separation of water between trees and streams in a Mediterranean climate, *Nat. Geosci.*, *3*, 100–104.

Broxton, P. D., P. A. Troch, and S. W. Lyon (2009), On the role of aspect to quantify water transit times in small mountainous catchments, *Water Resour. Res.*, *45*, W08427, doi:10.1029/2008WR007438.

Cardenas, M. B. (2007), Potential contribution of topography-driven regional groundwater flow to fractal stream chemistry: Residence time distribution analysis of Toth flow, *Geophys. Res. Lett.*, *34*, L05403, doi:10.1029/2006GL029126

Darracq, A., G. Destouni, K. Persson, C. Prieto, and J. Jarsjö (2010), Quantification of advective solute travel times and mass transport through hydrological catchments, *Environ. Fluid Mech.*, *10*, 103–120.

Destouni, G. (1991), Applicability of the steady-state flow assumption for solute advection in field soils, *Water Resour. Res.*, *27*, 2129–2140.

Destouni, G., and W. D. Graham (1995), Solute transport through an integrated heterogeneous soil-groundwater system, *Water Resour. Res.*, *31*, 1935–1944.

Destouni, G., G. Lindgren, and I. M. Gren (2006), Effects of inland nitrogen transport and attenuation modeling on coastal nitrogen load abatement, *Environ. Sci. Technol.*, *40*, 6208–6214.

Devroye, L. (1986), *Non-Uniform Random Variate Generation*, Springer, New York.

Fiori, A., and D. Russo (2008), Travel time distribution in a hillslope: Insight from numerical simulations, *Water Resour. Res.*, *44*, W12426, doi:10.1029/2008WR007135.

Harman, C., and M. Sivapalan (2009), A similarity framework to asses controls on shallow subsurface dynamics in hillslopes, *Water Resour. Res.*, *45*, W01417, doi:10.1029/2008WR007067.

Hrachowitz, M., C. Soulsby, D. Tetzlaff, J. J. C. Dawson, S. M. Dunn, and I. A. Malcolm (2009a), Using long-term data sets to understand transit times in contrasting headwater catchments, *J. Hydrol.*, *367*, 237–248.

Hrachowitz, M., C. Soulsby, D. Tetzlaff, J. J. C. Dawson, and I. A. Malcolm (2009b), Regionalization of transit time estimates in montane catchments by integrating landscape controls, *Water Resour. Res.*, *45*, W05421, doi:10.1029/2008WR007496.

Hrachowitz, M., C. Soulsby, D. Tetzlaff, I. A. Malcolm, and G. Schoups (2010), Gamma distribution models for transit time estimation in catchments: Physical interpretation of parameters and implications for time-variant transit time assessment, *Water Resour. Res.*, *46*, W10536, doi:10.1029/2010WR009148.

Hrachowitz, M., C. Soulsby, D. Tetzlaff, and I. A. Malcolm (2011), Sensitivity of mean transit time estimates to model conditioning and data availability, *Hydrol. Proc.*, *25*, 980–990.

Kirchner, J. W. (2003), A double paradox in catchment hydrology and geochemistry, *Hydrol. Process.*, *17*, 871–874.

Kirchner, J. W., X. Feng, and C. Neal (2000), Fractal stream chemistry and its implications for contaminant transport in catchments, *Nature*, *304*, 524–527.

Kreft, A., and A. Zuber (1978), On the physical meaning of the dispersion equation and its solutions for different initial and boundary conditions, *Chem. Eng. Sci.*, *33*, 1471–1480.

Lindgren G. A., G. Destouni, and A. V. Miller (2004), Solute transport through the integrated groundwater-stream system of a catchment, *Water Resour. Res.*, *40*, W03511, doi:10.1029/2003WR002765.

Lyon, S. W., S. L. E. Desilets, and P. A. Troch (2008), Characterizing the response of a catchment to an extreme rainfall event using hydrometric and isotopic data, *Water Resour. Res.*, *44*, W06413, doi:10.1029/2007WR006259.

Lyon, S. W., M. J. Mörth, C. Humborg, R. Giesler, and G. Destouni (2010), The relationship between subsurface hydrology and dissolved carbon fluxes for a sub-arctic catchment, *Hydrol. Earth Syst. Sci.*, *14*, 941–950.

McDonnell, J. J., et al. (2010), How old is streamwater? Open questions in catchment transit time conceptualization, modelling and analysis, *Hydrol. Process.*, *24*(12), 1745–1754.

McGuire, K. J., and J. J. McDonnell (2006), A review and evaluation of catchment transit time modeling, *J. Hydrol.*, *330*, 543–563.

McGuire, K. J., J. J. McDonnell, M. Weiler, C. Kendall, B. L. McGlynn, J. M. Welker, and J. Seibert (2005), The role of topography on catchment-scale water residence time, *Water Resour. Res.*, *41*, W05002, doi:10.1029/2004WR003657.

Niemi, A. J. (1977), Residence time distributions of variable flow processes, *Int. J. Appl. Radiat. Isot.*, *28*, 855–860.

Parker, J. C., and M. T. Van Genuchten (1984), Flux-averaged and volume-averaged concentrations in continuum approaches to solute transport, *Water Resour. Res.*, *20*, 866–872.

Persson, K., and G. Destouni (2009), Propagation of water pollution uncertainty and risk from the subsurface to the surface water system of a catchment, *J. Hydrol.*, *377*, 434–444, doi:10.1016/j.hydrol.2009.09.001.

Rinaldo, A., and M. Marani (1987), Basin Scale Model of Solute Transport. *Water Resour. Res.*, *23*, 2107–2118,

Rinaldo, A., K. J. Beven, E. Bertuzzo, L. Nicotina, J. Davies, A. Fiori, D. Russo, and G. Botter (2011), Catchment travel time distributions and waterflow in soils, *Water Resour. Res.*, *47*, W07537, doi:10.1029/2011WR010478.

Rozemeijer, J. C., Y. Van der Velde, F. C. Van Geer, G. H. De Rooij, P. J. J. F. Torfs, and H. P. Broers (2010), Improving load estimates for NO3 and P in surface waters by characterizing the concentration response to rainfall events, *Environ. Sci. Technol.*, *44*, 6305–6312.

Soulsby, C., D. Tetzlaff, and M. Hrachowitz (2009), Tracers and transit times: Windows for viewing catchment scale storage? *Hydrol. Process.*, *23*, 3503–3507.

Tetzlaff, D., J. Seibert, K. J. McGuire, H. Laudon, D. A. Burns, S. M. Dunn, and C. Soulsby (2009), How does landscape structure influence catchment transit time across different geomorphic provinces?, *Hydrol. Process.*, *23*, 945–953.

Tetzlaff, D., C. Soulsby, M. Hrachowitz, and M. Speed (2011), Relative influence of upland and lowland headwaters on the isotope hydrology and transit times of larger catchments, *J. Hydrol.*, *400*, 438–447.

Tiemeyer, B., B. Lennartz, and P. Kahle (2008), Analyzing nitrate losses from an artificially drained lowland catchment (North-Eastern Germany) with a mixing model, *Agric. Ecosyst. Environ.*, *123*, 125–136.

Van der Velde, Y., G. H. De Rooij, and P. J. J. F. Torfs (2009), Catchment-scale non-linear groundwater-surface water interactions in densely drained lowland catchments, *Hydrol. Earth Syst. Sci.*, *13*, 1867–1885.

Van der Velde, Y., G. H. de Rooij, J. C. Rozemeijer, F. C. van Geer, and H. P. Broers (2010a), The nitrate response of a lowland catchment: on the relation between stream concentration and travel time distribution dynamics, *Water Resour. Res.*, *46*, W11534, doi:10.1029/2010WR009105.

Van der Velde, Y., J. C. Rozemeijer, G. H. De Rooij, F. C. Van Geer, and H. P. Broers (2010b), Field-scale measurements for separation of catchment discharge into flow route contributions, *Vadose Zone J.*, *9*, 25–35, doi:10.2136/vzj2008.0141.

Van der Velde, Y., J. C. Rozemeijer, G. H. de Rooij, F. C. van Geer, and P. J. J. F. Torfs, and P. G. B. de Louw (2011), Improving catchment discharge predictions by inferring flow route contributions from a nested-scale monitoring and model setup, *Hydrol. Earth Syst. Sci.*, *15*, 913–930.

van Ommen, H. C., R. Dijksma, J. M. H. Hendrickx, L. W. Dekker, J. Hulshof, and M. van den Heuvel (1989a), Experimental assessment of preferential flow paths in a field soil, *J. Hydrol.*, *105*, 253–262.

Van Ommen, H. C., J. W. Hopmans, and S. E. A. T. M. van der Zee (1989b), Prediction of solute breakthrough from scaled soil physical properties, *J. Hydrol*, *105*, 263–273.

Visser, A., H. P. Broers, R. Heerdink, and M. F. P. Bierkens (2009), Trends in pollutant concentrations in relation to time of recharge and reactive transport at the groundwater body scale, *J. Hydrol.*, *369*, 427–439.

Wierenga, P. J. (1977), Solute distribution profiles computed with steady-state and transient water movement models, *Soil Sci. Soc. Am. J.*, *41*, 1050–1055.